ACS Catalysis

Research Article

pubs.acs.org/acscatalysis

A Cobalt Hydride Catalyst for the Hydrogenation of CO_2: Pathways for Catalysis and Deactivation

Matthew S. Jeletic, Monte L. Helm, Elliott B. Hulley, Michael T. Mock, Aaron M. Appel, and John C. Linehan*

Pacific Northwest National Laboratory, P.O. Box 999, MS K2-57, Richland, Washington 99352, United States

Supporting Information

ABSTRACT: The complex $Co(dmpe)_2H$ catalyzes the hydrogenation of CO_2 at 1 atm and 21 °C with significant improvement in turnover frequency relative to previously reported second- and third-row transition-metal complexes. New studies are presented to elucidate the catalytic mechanism as well as pathways for catalyst deactivation. The catalytic rate was optimized through the choice of the base to match the pK_a of the $[Co(dmpe)_2(H)_2]^+$ intermediate. With a strong enough base, the catalytic rate has a zeroth-order dependence on the base concentration and the pressure of hydrogen and a first-order dependence on the pressure of CO_2. However, for CO_2:H_2 ratios greater than 1, the catalytically inactive species $[(\mu\text{-dmpe})\text{-}(Co(dmpe)_2)_2]^{2+}$ and $[Co(dmpe)_2CO]^+$ were observed.

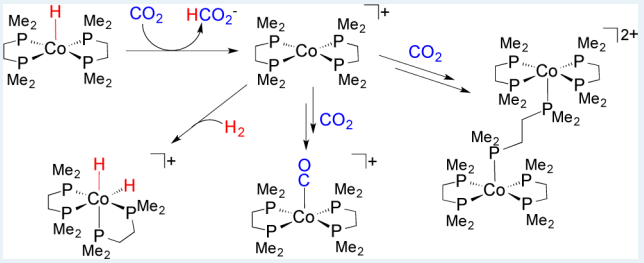

KEYWORDS: *CO_2, cobalt, hydrogenation, catalysis, high-pressure NMR*

INTRODUCTION

Increasing atmospheric CO_2 concentration and its link to climate change is a growing concern to the global community. Expanding the use of carbon-neutral energy sources, including solar and wind, will require energy storage, such as in the form of fuels.[1−4] Hydrogen is the simplest fuel, but using hydrogen for transportation remains a challenge because of its low volumetric energy density.[2,3,5] Carbon-based fuels such as methanol have higher volumetric energy densities but require the development of catalysts for their production.[2,3,5,6] One possible route for converting renewable hydrogen to carbon-based fuels is the hydrogenation of CO_2 to formate.

Haynes first reported catalytically reducing CO_2 to formamides in 1970,[7] and Inoue et al.[8] reported catalytic hydrogenation of CO_2 to formate in 1976 with Wilkinson's catalyst as well as nickel, iridium, ruthenium, and palladium phosphine complexes. Since these reports, much of the research on CO_2 reduction has focused on expensive transition metals such as ruthenium, iridium, and rhodium operating at temperatures and pressures usually exceeding 50 °C and 40 atm, respectively.[9−24] With varying degrees of success, a few research groups have demonstrated CO_2 hydrogenation using Ir- and Rh-based catalysts at room temperature but at elevated pressures, with turnover frequencies (TOFs) of up to 1335 h^{-1} and turnover numbers (TONs) of up to 7200.[25−31] Fujita, Himeda, and co-workers were able to demonstrate for the first time that a catalyst [hydroxybipyridyl($IrCp^*OH_2$)$_2$] could operate under ambient conditions with a TOF of <70 h^{-1}.[29−31] Nozaki and co-workers reported the most active catalyst to date, based on an Ir pincer complex, with TOFs and TONs reaching 150 000 h^{-1} and 3 500 000, respectively. However, these results were obtained at ≥49 atm and 120−200 °C, with dramatically increasing TOFs with increasing temperature.[32,33] Jessop and co-workers also reported a highly active ruthenium catalyst in supercritical CO_2 at 50 °C (TOF = 95 000 h^{-1}).[34]

Reports of hydrogenation of CO_2 to formate with first-row transition metals are relatively few in number[8,22,35−41] but are gaining significant attention. In 2003, Jessop and co-workers reported a high-pressure combinatorial approach for screening catalysts for CO_2 hydrogenation and therein reported that catalysts containing nonprecious metals were active for CO_2 hydrogenation.[36] They observed TOFs as high as 21 h^{-1} with TONs of 4400 (at 50 °C, 100 atm). In 2010, Beller and co-workers reported an iron tetraphosphine complex as a catalyst for the hydrogenation of CO_2 and followed this with a cobalt derivative in 2012, with TOFs of <65 h^{-1} and TONs of <1300 (100 °C, 10−90 atm).[37,39] Their recent work with iron catalysts improved the TOF to 255 h^{-1} and the TON to 5100 but still required high temperature and pressure (100 °C and 100 atm, respectively) under optimal conditions.[40] Milstein and co-workers[38] demonstrated hydrogenation of CO_2 with an iron compound based on a PNP pincer ligand analogous to that used by Nozaki and achieved TOFs and TONs as high as 156 h^{-1} and 788, respectively, at somewhat a milder pressure and temperature of 10 atm and 80 °C, respectively. Recently, Muckerman, Himeda, Fujita, and co-workers reported the complex $[Cp^*Co(III)(L)(DHBP)]^{n+}$ as a follow up to their Ir analogues.[41] The activity of 39 h^{-1} at 100 °C and 40 atm does

Received: July 11, 2014
Revised: August 25, 2014
Published: September 8, 2014

   dx.doi.org/10.1021/cs5009927 | ACS Catal. 2014, 4, 3755−3762

not compare favorably with those of their Ir complexes, but the catalyst is also able to operate in water.[41]

We previously reported a cobalt diphosphine complex capable of hydrogenating CO_2 under ambient conditions.[42] The TOF for this catalyst is comparable to those for the fastest catalysts for CO_2 hydrogenation reported to date and was measured under milder conditions (1−20 atm and 21 °C). Herein we report catalytic and mechanistic studies as well as deactivation pathways for this $Co(dmpe)_2H$ [dmpe = 1,2-bis(dimethylphosphino)ethane] catalyst system (Figure 1).

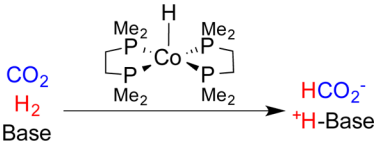

Figure 1. Reaction scheme for the production of formate from CO_2 and H_2.

RESULTS

Catalytic Hydrogenation of CO_2 with Verkade's Base. We previously reported $Co(dmpe)_2H$ as a catalyst for the hydrogenation of CO_2 to formate using 2,8,9-triisopropyl-2,5,8,9-tetraaza-1-phosphabicyclo[3.3.3]undecane (Verkade's base, Vkd) for the regeneration of this active hydride in the presence of H_2. Table 1 summarizes our results for CO_2 hydrogenation under a variety of conditions. The table is broken up into different subsections: entry 1 represents the standard conditions to which all other results are compared; entries 2 and 3 show the effect of varying the base concentration; entries 4 and 5 indicate the effects of changes in the total gas pressure; entries 6 and 7 contain the results obtained by starting from different catalytic intermediates; and finally, entries 8−11 reflect the results of varying the H_2:CO_2 ratio. Figures S1 and S2 in the Supporting Information are representative time-resolved multinuclear NMR spectra, and Figures S3−S5 are representative kinetic plots of the hydrogenation of CO_2 using $HCo(dmpe)_2$ in the presence of Verkade's base.

At the highest base concentration (Table 1, entry 3), the generated $[Vkd]+[HCO_2]^-$ salt exceeded its solubility limit in THF and precipitated after 2700 turnovers as measured by proton NMR spectroscopy. While the TOF for this run is accurate, the TON is not, and only an estimation of greater than 79% completion is possible.

At the highest pressure (20 atm), a lower catalyst concentration [0.040 mM $Co(dmpe)_2H$] was required in order to measure the high TOF of 74 000 ± 7500 h^{-1} (Table 1, entry 5), as the reaction went to completion too quickly to quantify at the typical catalyst concentration. However, the reaction was only 67% complete on the basis of quantification of the produced formate (TON of 9400) by ^1H NMR spectroscopy, even though the corresponding ^{31}P NMR spectrum confirmed that all of the Verkade's base was protonated (theoretical TON_{max} = 14 000). Spectroscopic characterization of the CO_2-derived products revealed the presence of two similar species: the formate and bicarbonate salts of protonated Verkade's base.

The formate salt of protonated Verkade's base, $[VkdH]^+[HCO_2]^-$, exhibits several distinct resonances by NMR and IR spectroscopies. In the ^1H NMR spectrum (Figure S6), the resonance for the formate proton is a singlet at 8.79 ppm and the P−H resonates as a doublet at 5.51 ppm (J_{P-H} = 500 Hz). The $^{31}P\{^1H\}$ spectrum exhibits a singlet at −12.9 ppm corresponding to the lone phosphorus (Figure S7). By exposure of a spent catalytic reaction to air and moisture, $[VkdH]^+[HCO_2]^-$ was transformed into $[VkdH]^+[HCO_3]^-$ over the course of a day. The $^{13}C\{^1H\}$ NMR (Figures S8 and S9) and IR spectra distinguished the two species. In the $^{13}C\{^1H\}$ spectra, the difference between the formate and bicarbonate carbon resonances was observed to be ∼10 ppm (166.3 and 157.6 ppm, respectively), and in the IR spectra, the C═O stretch changed by 20 wavenumbers (1611 and 1591 cm^{-1}, respectively). Furthermore, quantitative $^{13}C\{^1H\}$ NMR spectroscopy of a catalytic reaction mixture containing $[VkdH]^+[HCO_2]^-$ revealed a 1.1:1 ratio of $[HCO_2]^-$ to $[VkdH]^+$ (recycle time of 200 s). Multinuclear 2D HSQCAD NMR spectroscopy experiments confirmed that the signal at 8.79 ppm in the ^1H NMR spectrum corresponds to formate and not another species with a coincident resonance. Lastly, single-crystal X-ray diffraction studies confirmed the structures of $[VkdH]^+[HCO_2]^-$ (Figure S10 and Tables S1−S6) and $[VkdH]^+[HCO_3]^-$ (Figure S11 and Tables S7−S12).

Catalytic Hydrogenation of CO_2 with Other Bases. The CO_2 hydrogenation results are summarized in Table 2 for $Co(dmpe)_2H$, $[Co(dmpe)_2(H)_2]^+$, and $Rh(dmpe)_2H$, with a focus predominantly on 1,8-diazabicyclo[5.4.0]undec-7-ene

Table 1. Catalytic Conversion of CO_2 and H_2 to Formate with Co Complexes Using Verkade's Base[a]

entry	catalyst, conc. (mM)	conc. of base (mM)	P (atm), H_2:CO_2	TOF (h^{-1})	TON
1	$Co(dmpe)_2H$, 0.28	530	1.8, 50:50	6400 ± 600	1900[b]
2	$Co(dmpe)_2H$, 0.28	300	1.8, 50:50	4900 ± 500	1100
3	$Co(dmpe)_2H$, 0.28	950	1.8, 50:50	4900 ± 500	2700[c]
4	$Co(dmpe)_2H$, 0.28	570	1.0, 50:50	3400 ± 300	2100[b]
5	$Co(dmpe)_2H$, 0.040	510	20, 50:50	74000 ± 7500	9400[b,d]
6	$[Co(dmpe)_2(H)_2][BF_4]$, 0.26	520	1.8, 50:50	5200 ± 500	2100
7	$[Co(dmpe)_2][BF_4]$, 0.27	530	1.8, 50:50	4900 ± 500	2500
8	$Co(dmpe)_2H$, 0.28	530	1.8, 75:25	1000 ± 100	1600
9	$Co(dmpe)_2H$, 0.28	530	1.8, 65:35	2900 ± 300	2000
10	$Co(dmpe)_2H$, 0.28	530	1.8, 25:75	580 ± 60	410[e]
11	$Co(dmpe)_2H$, 0.28	520	1.2, 50:50	3200 ± 300	2000

[a]Catalytic conditions: 350−500 μL of THF-d_8, 1:1 CO_2:H_2, 21 °C, all reactions went to completion in 60 min or less, unless otherwise noted. [b]Previously reported.[42] [c][Vkd][formate] precipitated from solution before the reaction was complete, resulting in a 79% minimum conversion. [d]65% complete. [e]Catalyst decomposed. Vkd = 2,8,9-triisopropyl-2,5,8,9-tetraaza-1-phosphabicyclo[3.3.3]undecane. Uncertainties were derived from measured deviations in the NMR integrals; duplicate runs were within the uncertainty. See Figures S3−S5 for representative kinetic plots.

dx.doi.org/10.1021/cs5009927 | ACS Catal. 2014, 4, 3755−3762

Table 2. Catalytic Conversion of CO_2 and H_2 to Formate in the Presence of Other Bases[a]

entry	catalyst, conc. (mM)	base, conc (mM)	P (atm)	TOF (h^{-1})	TON
1	$Co(dmpe)_2H$, 36	DBU, 960	40	150 ± 15	61[b]
2	$Co(dmpe)_2H$, 42	DBU, 310	40	100 ± 10	47[b]
3	$Co(dmpe)_2H$, 38	DBU, 1270	40	180 ± 20	68[b]
4	$Co(dmpe)_2H$, 34	DBU, 1500	40	220 ± 20	73[b,c]
5	$Co(dmpe)_2H$, 41	DBU, 960	20	140 ± 15	59[b]
6	$Co(dmpe)_2H$, 42	DBU, 960	6.7	–[d]	7[b]
7	$Co(dmpe)_2H$, 42	DBU, 960	1.8	–[d]	7[b]
8	$[Co(dmpe)_2(H)_2]^+$, 32	DBU, 960	40	160 ± 15	73[b]
9	$Rh(dmpe)_2H$, 41	DBU, 960	40	16 ± 2	19[b,e]
10	$Rh(dmpe)_2H$, 130	DBU, 960	40	39 ± 4	13[b,e]
11	$Co(dmpe)_2H$, 40	NEt_3, 1000	40	–[d]	2
12	$Co(dmpe)_2H$, 2.8	P_1^tBu, 710	1.8	200 ± 20	150[f]
13	$Co(dmpe)_2H$, 3.8	P_1^tBu, 710	20	830 ± 80	110[f]
14	$Co(dmpe)_2H$, 3.8	P_1^tBu, 710	40	1400 ± 150	110[f]
15	$Co(dmpe)_2H$, 0.28	P_4^tBu, 400	1.8	6400 ± 650	1900

[a]Catalytic conditions: 300–500 μL of THF-d_8, 1:1 CO_2:H_2, 21 °C, reaction times less than 1 h, unless otherwise noted. [b]Consistent with a formate:DBU ratio of 2:1 from literature precedent.[43] [c]Incomplete reaction due to precipitation of formate. [d]After the initial monohydride was consumed, catalysis stopped. [e]Incomplete reaction (catalyst decomposed), 2 h reaction time. [f]Base decomposition occurred. DBU = 1,8-diazabicyclo[5.4.0]undec-7-ene, P_1^tBu = *tert*-butyliminotris(dimethylamino)phosphorane, P_4^tBu = 1-*tert*-butyl-4,4,4-tris(dimethylamino)-2,2-bis[tris(dimethylamino)phosphoranylidenamino]-2λ^5,4λ^5-catenadi(phosphazene).

(DBU) as the base. Entries 1–4 represent experiments with different concentrations of DBU; entries 5–7 show the dependence on the total gas pressure; entries 8–10 display the results using different catalysts; and finally, entries 11–15 illustrate the effects of using bases other than DBU (see Figures S12–S16 for representative time-resolved NMR spectra and kinetic plots).

Typical catalytic conditions consisted of 350–500 μL total volume of THF-d_8, 21 °C, 1:1 CO_2:H_2, 300–1500 mM base, and catalyst loadings of 10^{-5} to 10^{-7} mol (130–0.28 mM). The reported TONs in Table 2 are limited by the concentration of base, as most of the reactions went to completion as determined from the extent of conversion of the base to the corresponding protonated acid form (except entries 6, 7, and 11). In many cases, the TONs indicate a formate:protonated base ratio greater than 1 as a result of homoconjugation of formic acid and formate to generate an acid–base pair, as reported previously.[34,44] The extent of homoconjugation (and thus the maximum yield) varies with solvent, temperature, and the properties of the added base: DBU (2 in THF/21 °C),[34,43] NEt_3 (1.7),[34,36] P_4^tBu (1.5), Vkd (1.1), and P_1^tBu (1.5). For the catalytic hydrogenation of CO_2 to formate, the extent of homoconjugation must be understood to predict or understand the extent of conversion under specific conditions.

When the phosphazene base was used for the catalytic reaction (Figure S17), the ^1H NMR spectra initially displayed two resonances at 8.7 and 9.8 ppm, corresponding to formate and the protonated phosphazene base, respectively. Over the course of the catalytic reaction, the protic resonance of the iminophosphorane moved to overlap the formate resonance at 8.7 ppm. The ^{31}P NMR spectra (Figure S18) exhibited three resonances at 2.2, 25.0, and 37.1 ppm. The signals at 2.2 and 37.1 ppm correspond to the unprotonated and protonated phosphazene forms, respectively. The resonance at 25.0 ppm is the phosphine oxide, a known product of the reaction of the phosphazene base with CO_2.[45] In this experiment, the rate of the phosphazene reaction with CO_2 was lower than the rate of catalysis, but the observed TOF for formate production still provided the intended information relative to the base strength. The rate of base decomposition (induced by CO_2) appears to affect only the TON and not the TOF. Lastly, in all of the above studies, $Co(dmpe)_2H$ was not observed after introduction of the gases in either the ^1H or ^{31}P NMR spectra.

Control Experiments. In the absence of catalyst, no formate production was observed. Similarly, when no base was present, only stoichiometric formate conversion occurred. Adding H_2 (at 40 atm) to $Co(dmpe)_2H$ and $[Co(dmpe)_2(H)_2]^+$ resulted in no change in the ^1H or ^{31}P NMR spectra. The dihydride cation, $[Co(dmpe)_2(H)_2]^+$, also did not react with CO_2 (40 atm) or 1:1 CO_2:H_2 (40 atm). In contrast, $[Co(dmpe)_2]^+$ and $Co(dmpe)_2H$ quickly reacted with CO_2 (at 1 atm) to generate two new products (see the next section). The cobalt(II) precursors $[Co(CH_3CN)_6]^{2+}$ and $[Co(dmpe)_2(CH_3CN)]^{2+}$ were also tested for catalytic activity using Verkade's base and a 1:1 mixture of H_2 and CO_2. $[Co(CH_3CN)_6]^{2+}$ was noncatalytic even up to a total pressure of 40 atm. In contrast, $[Co(dmpe)_2(CH_3CN)]^{2+}$ was catalytic at a total pressure of 1.8 atm with a TOF similar to that for the analogous Co(I) complex. From additional studies, it was found that $[Co^{II}(dmpe)_2(CH_3CN)]^{2+}$ was converted into $Co^{I}(dmpe)_2H$ in the presence of Verkade's base under 1 atm H_2.

Low-temperature NMR spectroscopy investigations were undertaken to investigate possible initial species or previously unobserved intermediates. Reaction of $Co(dmpe)_2H$ with H_2/CO_2 at 1 atm and −40 °C demonstrated that the initial product of the reaction was a bound formate,[46] with a chemical shift of 8.17 ppm in the ^1H NMR spectrum. No evidence of a CO_2 bound to the cobalt was observed under these conditions. When the system was warmed to room temperature, the resonance shifted to the expected 8.79 ppm for unbound formate anion for the $[Co(dmpe)_2(H)_2]^+$ cation (Figures S19 and S20).

Nonproductive/Decomposition Pathways. For the cobalt complex, two predominant noncatalytic products were observed. The first was a yellow-colored product with a resonance at 53 ppm in the ^{31}P NMR spectrum, which was observed after complete consumption of the base (the rate of appearance appeared to depend on the catalyst concentration). The second product was a THF-insoluble orange precipitate

dx.doi.org/10.1021/cs5009927 | ACS Catal. 2014, 4, 3755–3762

observed when the CO_2:H_2 ratio was greater than 1. When redissolved in CD_3CN, this precipitate exhibited two resonances at −13 and 54 ppm (1:4 ratio) in the $^{31}P\{^1H\}$ NMR spectrum. For comparison, the resonances of yellow-colored $Co(dmpe)_2H$, colorless $[Co(dmpe)_2(H)_2]^+$, and red-brown $[Co(dmpe)_2]^+$ occur at 48, 52/61, and 49 ppm, respectively. Also, neither of the two new species appeared to contain resonances attributable to hydride species in the ^1H NMR spectra. We propose the yellow product and orange precipitate to be a monocarbonyl species and a dimer, respectively (illustrated in Figure 2).

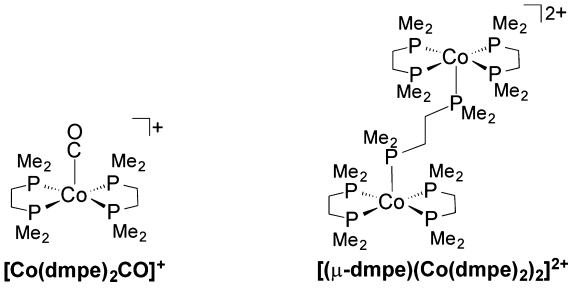

Figure 2. Proposed products from the reaction of $Co(dmpe)_2H$ with excess CO_2.

The dimeric species $[(\mu\text{-dmpe})(Co(dmpe)_2)_2]^{2+}$ is insoluble in THF and therefore catalytically inactive under the reaction conditions. As described above, at 1.8 atm (4:1 CO_2:H_2) only limited catalysis occurred because of the formation of an orange precipitate. In addition to these observations, analysis of the headspace gas from a mixture of $Co(dmpe)_2H$ and CO_2 after 5 min revealed a significant amount of CO as well as the expected CO_2 in an approximately 1:5 ratio with only a trace of H_2. For comparison, the reaction of $[Co(dmpe)_2]^+$ with 0.5 equiv of ammonium formate (in the absence of CO_2) yielded a mixture of all of the species in Figures 2 and 4, as illustrated by the NMR spectrum in Figure 3.

To confirm the identity of $[(\mu\text{-dmpe})(Co(dmpe)_2)_2]^{2+}$, an authentic sample was synthesized for comparison by NMR spectroscopy. Upon reaction of $Co(dmpe)_2H$ with CO_2 at 1 atm, the solution immediately turned from orange to red followed by the formation of an orange precipitate, indicative of the conversion of $Co(dmpe)_2H$ into $[Co(dmpe)_2]^+$ before the formation of $[(\mu\text{-dmpe})(Co(dmpe)_2)_2]^{2+}$. After removal of the solvent by vacuum, the resulting solid was dissolved in CD_3CN and gave the same ^{31}P resonances (54 and −13, 4:1 ratio) as the species generated under catalytic conditions with a high CO_2:H_2 ratio. In addition, resonances attributable to $[Co(dmpe)_2CO]^+$ were also present (Figure S21). Repeating this experiment except using $[Co(dmpe)_2]^+$ in place of the hydride provided similar results. Diffusion of diethyl ether into the reaction mixture resulted in the formation of crystals that yielded a structure with two bis(diphosphine)cobalt complexes linked by a dmpe ligand (Figures S22 and S23). Furthermore, addition of 0.5 equiv of dmpe to $[Co(dmpe)_2]^+$ in acetonitrile yielded the same resonances in the ^{31}P NMR spectrum, consistent with the orange precipitate formed during catalysis.

On the basis of the observed generation of CO and the fact that $[Co(dmpe)_2]^+$ is a coordinatively unsaturated 16-electron complex, we postulate that $[Co(dmpe)_2CO]^+$ can form. Treating $Co(dmpe)_2H$ with a 1:1 mixture of CO_2 and H_2 in the absence of added base eventually formed the cobalt carbonyl

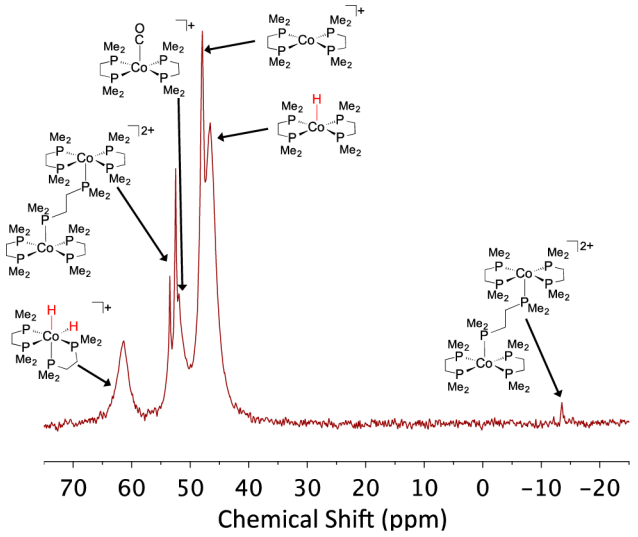

Figure 3. $^{31}P\{^1H\}$ NMR spectrum of $[Co(dmpe)_2]^+$ following the addition of 0.5 equiv of ammonium formate..

complex and a stoichiometric amount of formate. The $[Co(dmpe)_2]^+$ intermediate was not observed because it immediately reacted with H_2 to generate the dihydride, $[Co(dmpe)_2(H)_2]^+$. After 1 h, the dihydride began to slowly convert to $[Co(dmpe)_2CO]^+$, possibly through a reaction involving the formate anion. Accompanying this reaction, the solution changed from orange to colorless, then slowly converted to yellow, and finally darkened. After 60 days in a sealed J. Young tube at 21 °C, more than 95% of the cobalt complex converted to the $[Co(dmpe)_2CO]^+$ complex. The $^{13}C\{^1H\}$ NMR spectrum (Figure S24) exhibited a resonance at 203 ppm and the IR spectrum (Figure S25) displayed a peak at 1905 cm^{-1} indicating a Co−CO bond, in agreement with results for other reported bis(diphosphine)cobalt−carbonyl complexes.[47−51] The IR spectrum also displayed a signal at 1606 cm^{-1} corresponding to an organic carbonyl, consistent with the formate counterion.

The conversion to $[Co(dmpe)_2CO]^+$ appeared to be related to the number of equivalents of formate present: specifically, at higher relative concentrations of formate, conversion to $[Co(dmpe)_2CO]^+$ occurred more quickly. Following catalytic hydrogenation of CO_2 to formate, $[Co(dmpe)_2CO]^+$ was the only cobalt phosphine species observable by $^{31}P\{^1H\}$ NMR spectroscopy after 24 h, whereas 60 days was necessary for complete conversion following the noncatalytic reaction of CO_2 and the cobalt hydride. Consistent with the generation of catalytically inactive species, addition of more base after 24 h yielded no further catalytic activity (Figure S26), suggesting that the proposed cobalt species, $[Co(dmpe)_2CO]^+$, is catalytically inactive under these conditions. For comparison, reaction of $[Co(dmpe)_2]^+$ with 1 atm ^{13}CO generated a number of Co−CO species within minutes, with the $^{13}C\{^1H\}$ NMR spectrum displaying four resonances between 203 and 206 ppm (Figure S27). The $^{31}P\{^1H\}$ NMR spectrum (Figure S28) also indicated that CO displaced dmpe from the metal, which could provide the source for the bridging dmpe ligand in $[(\mu\text{-dmpe})(Co(dmpe)_2)_2]^{2+}$, the bimetallic complex that was also observed.

DISCUSSION

In our previous report on CO_2 hydrogenation,[42] we proposed the cycle illustrated in Figure 4,[26,27,42,52,53] and here we report

dx.doi.org/10.1021/cs5009927 | ACS Catal. 2014, 4, 3755−3762

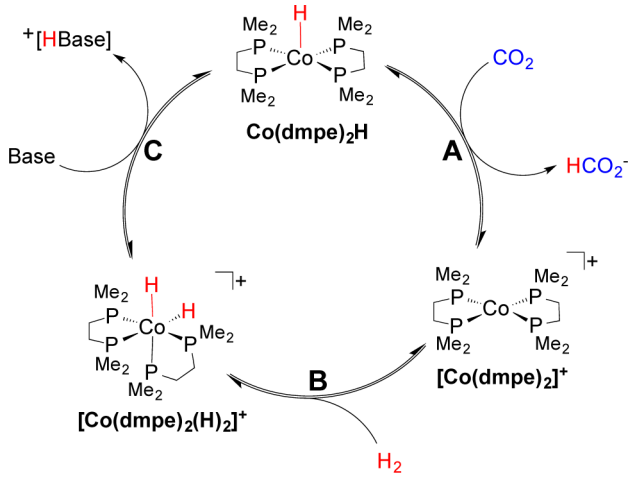

Figure 4. Proposed catalytic cycle for hydrogenation of CO_2 with $Co(dmpe)_2H$.

more detailed supporting evidence for this mechanism as well as modes of catalyst deactivation. Consistent with the proposed mechanism, the same TOF was observed when starting from any of the three intermediates displayed in Figure 4. Our preliminary studies suggested that the pK_a of the base influenced the rate-determining step and, by extension, the rate of reaction; however, with Verkade's base, the rate was independent of base concentration. Consistent with these results, in operando ^{31}P and ^{1}H NMR spectroscopy revealed $Co(dmpe)_2H$ as the only observable steady-state intermediate in the presence of Verkade's base, whereas $[Co(dmpe)_2(H)_2]^+$ and $[Co(dmpe)_2]^+$ were not observed. This observation suggests that step A in Figure 4 is the rate-determining step,[46] and on the basis of available thermochemical data, this step is expected to be downhill by approximately 8 kcal/mol.[42,54−57] Therefore, the reverse reaction is not expected to occur to a significant extent, resulting in the simple rate law shown in eq 1. Thus, under the experimental conditions for the catalytic studies, the reaction should be independent of both the base concentration and the hydrogen pressure.

$$\text{rate} = k_A[CO_2][\text{catalyst}] \quad (1)$$

Experiments to determine the dependence on the base concentration and hydrogen pressure yielded results that are consistent with the rate law in eq 1. However, increasing the CO_2:H_2 ratio to above 1 did not lead to an enhancement in rate but rather resulted in the observation of side reactions that appeared to correspond to generation of CO. Two likely routes to the formation of CO are the reverse water-gas shift (eq 2) and formate dehydroxylation (eq 3). Presumably, formate dehydroxylation could occur at any gas ratio, so on the basis of the fact that CO formation only occurred at higher CO_2:H_2 ratios, the reverse water-gas shift is expected to be the more likely pathway for generation of CO.

$$H_2 + CO_2 \rightarrow H_2O + CO \quad (2)$$

$$HCO_2^- \rightarrow OH^- + CO \quad (3)$$

The introduction of water enabled a competing reaction to occur, specifically the reaction of CO_2, water, and base to generate bicarbonate and protonated base. This competition between formate and bicarbonate production favors the formation of bicarbonate at higher concentrations of water. In general, the water content had to exceed 30 ppm (as measured by Karl Fischer titration) before the formation of bicarbonate occurred to an appreciable extent under the conditions used for catalysis. For limited amounts of bicarbonate, the formation of bicarbonate was observed by $^{13}C\{^1H\}$ NMR spectroscopy following completion of the catalytic reaction (the acquisition times necessary for quantitative $^{13}C\{^1H\}$ NMR spectra were too long for in operando observation). For extensive formation of bicarbonate, a significant amount of precipitate was observed. This precipitate, the salt of the protonated base and bicarbonate, was readily observable and also corresponded with broadening of all of the resonances in the ^1H NMR spectrum. The white solid isolated from the reaction mixture evolved gas upon reaction with acid, also consistent with the formation of bicarbonate.

Experiments using bases with lower pK_a values yielded results that support the catalytic cycle displayed in Figure 4. With weaker bases, step C in the catalytic cycle, deprotonation of the Co(III) dihydride, is expected to limit the catalytic rate. Consistent with this expectation, only $[Co(dmpe)_2(H)_2]^+$ was observed using in operando NMR spectroscopy. In the presence of DBU at a pressure of 40 atm, $Co(dmpe)_2H$ produced a modest TOF of 145 h^{-1}, which is still comparable to the results for other first-row transition-metal catalysts.[8,35−41] As the concentration of DBU increased, the TOF also increased. This correlation is expected considering that adding more base shifts the equilibrium in step C of the catalytic cycle from $[Co(dmpe)_2(H)_2]^+$ to $Co(dmpe)_2H$. The catalyst TOF was observed to have a first-order dependence on the concentration of DBU (Figure S29). Oddly, all of the kinetic profiles with DBU as the base displayed a minimum induction period of 15 min. We did not observe this induction period with any of the other bases. Furthermore, when the concentration of DBU reached 1500 mM, the induction period increased to 40 min, and above that concentration the induction period exceeded 2 h. The longer induction period may merely be a consequence of the increasing viscosity of the solution with increasing concentration of DBU, thereby hindering gas−liquid mixing. Alternatively, DBU could competitively bind to a cobalt intermediate in the catalytic cycle, most likely $[Co(dmpe)_2]^+$. No direct observation of the latter occurred for the cobalt−dmpe complexes in this study. A third possibility is the presence of an unknown (and unmeasured) impurity in the DBU that inhibits one of the reaction steps until the impurity is consumed.

Because of the dependence of the catalytic TOF on the concentration of DBU, the dependence on the strength of the base was further explored. In CH_3CN, the pK_a values for the conjugate acids of the bases used are known, including triethylamine (pK_a = 18.8),[58] DBU (pK_a = 24.3),[58] *tert*-butyliminotris(dimethylamino)phosphorane (P_1^tBu) (pK_a = 27.0),[58] Verkade's base (pK_a = 33.6),[59] and 1-*tert*-butyl-4,4,4-tris(dimethylamino)-2,2-bis[tris(dimethylamino)phosphoranylidenamino]-2λ^5,4λ^5-catenadi(phosphazene) (P_4^tBu) (pK_a = 42.6).[60] The weakest base, triethylamine, resulted only in stoichiometric hydride transfer, even at 40 atm. The TOFs under similar conditions were 150 h^{-1} for DBU, 1400 h^{-1} for P_1^tBu, and 74 000 h^{-1} for Verkade's base. Use of a stronger base than Verkade's base, P_4^tBu, did not increase the TOF. Again, this is consistent with the proposed mechanism and eq 1, specifically that the rate is independent of the base concentration or identity when the pK_a for the conjugate acid is equal to or greater than the pK_a of $[Co(dmpe)_2(H)_2]^+$. The observed TOFs as a function of basicity demonstrate the expected trend that the TOF increases with increasing pK_a of the conjugate acid of the base.

dx.doi.org/10.1021/cs5009927 | ACS Catal. 2014, 4, 3755−3762

Most of the studies using different bases have focused on the effect of basicity. However, the effect of gas pressure on the TOF for weaker bases is also of interest. When DBU is used as the base, there is no difference in TOF at 40 and 20 atm, and the reaction becomes noncatalytic at lower pressures. In contrast, using the phosphazene base P_1^tBu, we observed a first-order dependence on the total gas pressure from 1.8 to 40 atm, with a second-order rate constant of 9.7×10^{-4} atm^{-1} s^{-1} (Figure S30). These data suggest that pressure begins to contribute more to the overall rate as the pK_a of the base becomes better matched to the pK_a of the metal dihydride. The overall rate constant appears to be a composition of the equilibrium constant for step C and the rate constant for step A in Figure 4. This finding also explains why the reaction catalyzed by the analogous species $Rh(dmpe)_2H$ is an order of magnitude slower than that catalyzed by $Co(dmpe)_2H$, as the increase in driving force for the hydride transfer (step A) is offset by the decrease in acidity of the dihydride (pertinent to step C). For this rhodium complex, the pK_a is approximately 3 higher than that for the analogous cobalt complex on the basis of previous computational studies.[61]

Beller and co-workers previously reported a cobalt(II) species as the active catalyst for CO_2 hydrogenation.[39] Under the conditions used in this study, attempts to verify a cobalt(II) intermediate starting from $[Co(dmpe)_2(CH_3CN)]^{2+}$ led to catalysis with TOFs similar to those for the cobalt(I) hydride, $Co(dmpe)_2H$. However, in the presence of 1 atm H_2 and excess Verkade's base, $[Co(dmpe)_2(CH_3CN)]^{2+}$ nearly quantitatively converts into $Co(dmpe)_2H$. This transformation presumably occurs through the initial conversion of the cobalt(II) complex to the cobalt(II) hydride and a protonated base by heterolytic cleavage of H_2. The cobalt(II) hydride can then undergo hydrogen-atom transfer to another cobalt(II) hydride to generate $[Co(I)(dmpe)_2]^+$ and $[Co(III)(dmpe)_2H_2]^+$, as illustrated in Figure 5. Consistent with steps B and C in Figure 4, $[Co(I)(dmpe)_2]^+$ can then add H_2 to yield a second equivalent of $[Co(III)(dmpe)_2H_2]^+$, both of which can be deprotonated by Verkade's base to generate the monohydride. DuBois and co-workers previously reported a similar disproportionation of $Co(dppe)_2H$.[62] This method provides a much cleaner, higher-yielding synthetic route to obtain $Co(dmpe)_2H$.

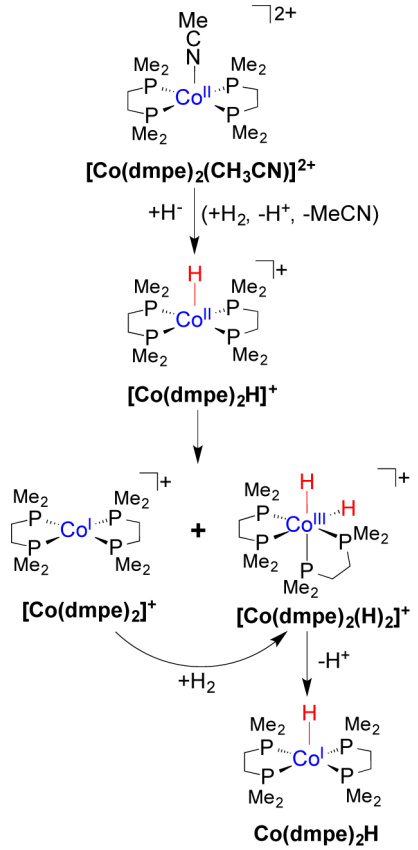

Figure 5. Proposed route for the conversion of the precursor $[Co(II)(dmpe)_2]^{2+}$ into the active catalyst $Co(dmpe)_2H$.

SUMMARY AND CONCLUSIONS

$Co(dmpe)_2H$ is an effective catalyst for the hydrogenation of CO_2 to formate. In the presence of Verkade's base and a 1:1 mixture of CO_2 and H_2, TOFs of 3400 and 74 000 h^{-1} were measured at 1 and 20 atm, respectively. The TOF is first-order in the total gas pressure. On the basis of in operando NMR spectroscopy measurements as well as studies in which the CO_2:H_2 ratio was varied, the TOF appears to be first-order in the CO_2 pressure and independent of the H_2 pressure. With Verkade's base, the TOF does not depend on the concentration of base, but a first-order dependence on the concentration of base was observed with weaker bases such as DBU.

A deactivation pathway was observed in which a carbon monoxide complex is formed. The CO complex was observed to form quickly in the presence of higher CO_2:H_2 ratios. This observation is consistent with a reaction analogous to the reverse water-gas shift, possibly related to the unobserved binding of CO_2 to $[Co(dmpe)_2]^+$. Using higher CO_2:H_2 ratios appears to make this deactivation pathway competitive with addition of H_2.

$Co(dmpe)_2H$ was found to have the highest catalytic activity with Verkade's base but still had significant activity with weaker bases such as DBU. The rates observed with DBU are comparable to those with other catalysts based on cobalt complexes that have been reported. Improvements in the present catalyst may be possible through variation of the diphosphine ligands. Increasing the acidity of the dihydride may lead to improvements in the catalytic performance, specifically by enabling the use of weaker bases. These studies are currently underway in our laboratories.

EXPERIMENTAL SECTION

Materials and Methods. All manipulations were performed under an atmosphere of N_2 unless stated otherwise. The phosphazene bases and Verkade's base were purchased from Sigma-Aldrich and used without further purification. Triethylamine and DBU were dried over sodium and 4 Å sieves until the water content was below 20 ppm, as determined by Karl Fischer titration. THF-d_8, CD_3CN, and DMSO-d_6 were ordered from Cambridge Isotope Laboratories. THF-d_8 was dried over NaK, and CD_3CN was dried over calcium hydride. Headspace gas was measured by gas chromatography using a 10 ft. by 1/8 in. 100/120 Carbosieve S–II stainless steel column purchased from Supelco in an Agilent Technologies model 6850 chromatograph. A thermal conductivity detector was used, and the oven temperature was ramped from 100 to 175 °C with argon as the carrier gas at a flow rate of 15 mL/min.

The syntheses of $Co(dmpe)_2H$, $[Co(dmpe)_2(H)_2]BF_4$, $[Co(dmpe)_2]BF_4$, and $Rh(dmpe)_2H$ are reported elsewhere.[54,63] Because of the reactivity of $Rh(dmpe)_2H$, it was prepared immediately before use.[54] Gases were UHP-grade or better. The

dx.doi.org/10.1021/cs5009927 | ACS Catal. 2014, 4, 3755–3762

gas was delivered to the NMR tube directly from the tank through a stainless steel gas manifold line at pressures less than 1.8 atm and by an ISCO pump at pressures greater than 6.7 atm. The PEEK high-pressure NMR tubes were designed and built at Pacific Northwest National Laboratory.[64,65] The capillary standard was prepared by adding $Co(NO_3)_2$ to D_2O until the resonance in the ^1H NMR spectrum of the residual HDO resonance appeared at a desirable location.

Representative Preparation in a J. Young Glass NMR Tube. A glass capillary containing the standard was added to the tube. Verkade's base was dissolved in 200 μL of THF-d_8 and then added to the tube, followed by 50 μL of the catalyst solution at the desired dilution. The tube was then filled to a total volume of 500 μL with THF-d_8, sealed, and transferred to the gas manifold line. A pseudo-freeze–pump–thaw method was used to eliminate N_2 from the tube. The CO_2/H_2 gas mixture was delivered, and the system was mixed for 30 s on a vortex mixer before the NMR spectrum was collected. The tube was then reconnected to the gas manifold, and after the gas was removed from the headspace, fresh gas was added. These steps were repeated until the reaction was complete. Figure S31 shows that under the above conditions, the reaction required just over 5 min for complete gas consumption at 1.8 atm. The length of time elapsed between each refill was approximately 2 min.

Representative Sample Preparation in a PEEK Tube. A glass capillary containing the standard was added to the tube. The base was dissolved in 150 μL of THF-d_8 and then added to the tube, followed by 50 μL of the catalyst at the desired dilution. The tube was then filled to a total volume of between 330 and 390 μL with THF-d_8, sealed, and transferred a high-pressure manifold equipped with an ISCO pump. A pseudo-freeze–pump–thaw method was used to eliminate N_2 from the tube, and then the CO_2/H_2 gas mixture was delivered at a constant pressure by an ISCO pump at the desired pressure. The NMR tube was placed on a vortex mixer to allow for gas mixing. NMR spectra were collected 2–5 min apart. When the PEEK NMR tube was not in the spectrometer, it was again agitated using a vortex mixer.

Acquisition of NMR Spectra. Proton NMR spectra were collected at 500 MHz on a Varian spectrometer with a 13° pulse, an acquisition time of 2 s, and a recycle time of 1 s; the total acquisition time for one transient was 3 s. Either eight or 16 transients were collected for each cycle for a total NMR acquisition time of 24 or 48 s. Spectra were referenced to internal residual protonated solvent. These parameters were found to yield reproducible quantitative results under the reaction conditions listed through testing with known concentrations of formate-containing solutions. At high catalyst concentration, the sealed D_2O standard was integrated against the cobalt hydride resonance before addition of gases. At low catalyst concentration, the hydride resonance was not observable and an external calibration of the sealed D_2O standard was used. As an additional internal standard, the area of the proton NMR resonance of the acidic proton of protonated Verkade's base (which is split into two resonances by scalar coupling from ^{31}P) was also used. During experiments for collecting kinetic data, minimal shimming was used before spectral collection, and the sample was run without spinning to minimize the time between cycles. The time specified for each cycle was from the start of the first transient. Turnover frequencies were calculated from the slope of the linear portion of the kinetic curves such as those displayed in Figures S3–S5. The TOFs listed in Table 1 are averages of two to three experiments run under the same conditions. In addition, in an attempt to eliminate effects from gas–liquid mixing, the catalyst concentration was decreased until a nearly constant TOF was obtained for two subsequent concentrations. $^{31}P\{^1H\}$ NMR spectra were collected at time zero, selected times during the reaction, and after catalysis was complete. Spectra were referenced to external phosphoric acid.

X-ray Experimental Details. Single crystals of $[VkdH]^+[HCO_3]^-$ were grown in THF to yield long white needles. A suitable crystal was selected and mounted using Paratone N on a nylon fiber on a Bruker APEX-II CCD diffractometer. The crystal was kept at 143.15 K during data collection. Using Olex2,[66] the structure was solved with the SHELXS[67] structure solution program using direct methods and refined with the SHELXL[67] refinement package using least-squares minimization. Crystal data: $C_{16}H_{39}N_4O_5P$, M = 398.48, triclinic, a = 8.8946(19) Å, b = 9.599(2) Å, c = 14.595(3) Å, α = 105.460(6)°, β = 94.446(6)°, γ = 114.780(6)°, V = 1064.5(4) Å^3, T = 143 K, space group $P\bar{1}$ (no. 2), Z = 2, μ(Mo Kα) = 0.161, 18 554 reflections measured, 5060 unique (R_{int} = 0.0769) which were used in all calculations. The final wR_2 was 0.1909 (all data), and R_1 was 0.0684 [$I > 2\sigma(I)$].

Single crystals of $[VkdH]^+[HCO_2]^-$ were grown by slow evaporation of hexane into THF. A suitable crystal was selected and mounted on a nylon fiber using Paratone N oil on a Bruker APEX-II CCD diffractometer. The crystal was kept at 145 K during data collection. Using Olex2,[66] the structure was solved with the SHELXS[67] structure solution program using the Patterson method and refined with the SHELXL[67] refinement package using least-squares minimization. Crystal data: $C_{16}H_{35}N_4O_2P$, M = 346.45, triclinic, a = 9.420(8) Å, b = 10.0652(9) Å, c = 11.6878(10) Å, α = 72.135(2)°, β = 84.493(3)°, γ = 64.509(2)°, V = 958.49(14) Å^3, T = 145 K, space group $P\bar{1}$ (no. 2), Z = 2, μ(Mo Kα) = 0.158, 22 542 reflections measured, 6295 unique (R_{int} = 0.0303) which were used in all calculations. The final wR_2 was 0.1222 (all data), and R_1 was 0.0448 [$I > 2\sigma(I)$].

■ ASSOCIATED CONTENT

Supporting Information

Kinetic plots, NMR spectroscopy data, IR spectroscopy data, and crystallographic data (CIF). This material is available free of charge via the Internet at http://pubs.acs.org.

■ AUTHOR INFORMATION

Corresponding Author

*E-mail: john.linehan@pnnl.gov.

Notes

The authors declare no competing financial interest.

■ ACKNOWLEDGMENTS

Research by M.S.J., M.T.M., A.M.A., and J.C.L. was supported by the U.S. Department of Energy, Office of Basic Energy Sciences, Division of Chemical Sciences, Geosciences, and Biosciences. Research by M.L.H. and E.B.H. was supported as part of the Center for Molecular Electrocatalysis, an Energy Frontier Research Center funded by the U.S. Department of Energy, Office of Science. Pacific Northwest National Laboratory (PNNL) is a multiprogram national laboratory operated for the DOE by Battelle.

■ REFERENCES

(1) Savéant, J.-M. *Chem. Rev.* **2008**, *108*, 2348–2378.
(2) Benson, E. E.; Kubiak, C. P.; Sathrum, A. J.; Smieja, J. M. *Chem. Soc. Rev.* **2009**, *38*, 89–99.
(3) Cook, T. R.; Dogutan, D. K.; Reece, S. Y.; Surendranath, Y.; Teets, T. S.; Nocera, D. G. *Chem. Rev.* **2010**, *110*, 6474–6502.

(4) Thoi, V. S.; Sun, Y.; Long, J. R.; Chang, C. J. *Chem. Soc. Rev.* **2013**, *42*, 2388−2400.
(5) Appel, A. M.; Bercaw, J. E.; Bocarsly, A. B.; Dobbek, H.; DuBois, D. L.; Dupuis, M.; Ferry, J. G.; Fujita, E.; Hille, R.; Kenis, P. J. A.; Kerfeld, C. A.; Morris, R. H.; Peden, C. H. F.; Portis, A. R.; Ragsdale, S. W.; Rauchfuss, T. B.; Reek, J. N. H.; Seefeldt, L. C.; Thauer, R. K.; Waldrop, G. L. *Chem. Rev.* **2013**, *113*, 6621−6658.
(6) Olah, G. A.; Prakash, G. K. S.; Goeppert, A. *J. Am. Chem. Soc.* **2011**, *133*, 12881−12898.
(7) Haynes, P.; Slaugh, L. H.; Kohnle, J. F. *Tetrahedron Lett.* **1970**, *11*, 365−368.
(8) Inoue, Y.; Izumida, H.; Sasaki, Y.; Hashimoto, H. *Chem. Lett.* **1976**, 863−864.
(9) Wang, W.; Wang, S.; Ma, X.; Gong, J. *Chem. Soc. Rev.* **2011**, *40*, 3703−3727.
(10) Wesselbaum, S.; vom Stein, T.; Klankermayer, J.; Leitner, W. *Angew. Chem., Int. Ed.* **2012**, *51*, 7499−7502.
(11) Cokoja, M.; Bruckmeier, C.; Rieger, B.; Herrmann, W. A.; Kühn, F. E. *Angew. Chem., Int. Ed.* **2011**, *50*, 8510−8537.
(12) Federsel, C.; Jackstell, R.; Beller, M. *Angew. Chem., Int. Ed.* **2010**, *49*, 6254−6257.
(13) Jessop, P. G.; Ikariya, T.; Noyori, R. *Chem. Rev.* **1995**, *95*, 259−272.
(14) Jessop, P. G.; Joó, F.; Tai, C.-C. *Coord. Chem. Rev.* **2004**, *248*, 2425−2442.
(15) Leitner, W. *Angew. Chem., Int. Ed. Engl.* **1995**, *34*, 2207−2221.
(16) Azua, A.; Sanz, S.; Peris, E. *Chem.—Eur. J.* **2011**, *17*, 3963−3967.
(17) Maenaka, Y.; Suenobu, T.; Fukuzumi, S. *Energy Environ. Sci.* **2012**, *5*, 7360.
(18) Himeda, Y.; Onozawa-Komatsuzaki, N.; Sugihara, H.; Kasuga, K. *Organometallics* **2007**, *26*, 702−712.
(19) Schmeier, T. J.; Dobereiner, G. E.; Crabtree, R. H.; Hazari, N. *J. Am. Chem. Soc.* **2011**, *133*, 9274−9277.
(20) Ogo, S.; Kabe, R.; Hayashi, H.; Harada, R.; Fukuzumi, S. *Dalton Trans.* **2006**, 4657−4663.
(21) Hayashi, H.; Ogo, S.; Fukuzumi, S. *Chem. Commun.* **2004**, 2714.
(22) Drake, J. L.; Manna, C. M.; Byers, J. A. *Organometallics* **2013**, *32*, 6891−6894.
(23) Huff, C. A.; Sanford, M. S. *ACS Catal.* **2013**, *3*, 2412−2416.
(24) Sanz, S.; Azua, A.; Peris, E. *Dalton Trans.* **2010**, *39*, 6339−6343.
(25) Ezhova, N. N.; Kolesnichenko, N. V.; Bulygin, A. V.; Slivinskii, E. V.; Han, S. *Russ. Chem. Bull., Int. Ed.* **2002**, *51*, 2165−2169.
(26) Graf, E.; Leitner, W. *J. Chem. Soc., Chem. Commun.* **1992**, 623−624.
(27) Gassner, F.; Leitner, W. *J. Chem. Soc., Chem. Commun.* **1993**, 1465.
(28) Angermund, K.; Baumann, W.; Dinjus, E.; Fornika, R.; Görls, H.; Kessler, M.; Krüger, C.; Leitner, W.; Lutz, F. *Chem.—Eur. J.* **1997**, *3*, 755−764.
(29) Hull, J. F.; Himeda, Y.; Wang, W.-H.; Hashiguchi, B.; Periana, R.; Szalda, D. J.; Muckerman, J. T.; Fujita, E. *Nat. Chem.* **2012**, *4*, 383−388.
(30) Wang, W.-H.; Hull, J. F.; Muckerman, J. T.; Fujita, E.; Himeda, Y. *Energy Environ. Sci.* **2012**, *5*, 7923−7926.
(31) Wang, W.-H.; Muckerman, J. T.; Fujita, E.; Himeda, Y. *ACS Catal.* **2013**, *3*, 856−860.
(32) Tanaka, R.; Yamashita, M.; Nozaki, K. *J. Am. Chem. Soc.* **2009**, *131*, 14168−14169.
(33) Tanaka, R.; Yamashita, M.; Chung, L. W.; Morokuma, K.; Nozaki, K. *Organometallics* **2011**, *30*, 6742−6750.
(34) Munshi, P.; Main, A. D.; Linehan, J. C.; Tai, C.-C.; Jessop, P. G. *J. Am. Chem. Soc.* **2002**, *124*, 7963−7971.
(35) Evans, G. O.; Newell, C. J. *Inorg. Chim. Acta* **1978**, *31*, L387−L389.
(36) Tai, C.-C.; Chang, T.; Roller, B.; Jessop, P. G. *Inorg. Chem.* **2003**, *42*, 7340−7341.
(37) Federsel, C.; Boddien, A.; Jackstell, R.; Jennerjahn, R.; Dyson, P. J.; Scopelliti, R.; Laurenczy, G.; Beller, M. *Angew. Chem., Int. Ed.* **2010**, *49*, 9777−9780.
(38) Langer, R.; Diskin-Posner, Y.; Leitus, G.; Shimon, L. J. W.; Ben-David, Y.; Milstein, D. *Angew. Chem., Int. Ed.* **2011**, *50*, 9948−9952.
(39) Federsel, C.; Ziebart, C.; Jackstell, R.; Baumann, W.; Beller, M. *Chem.—Eur. J.* **2012**, *18*, 72−75.
(40) Ziebart, C.; Federsel, C.; Anbarasan, P.; Jackstell, R.; Baumann, W.; Spannenberg, A.; Beller, M. *J. Am. Chem. Soc.* **2012**, *134*, 20701−20704.
(41) Badiei, Y. M.; Wang, W.-H.; Hull, J. F.; Szalda, D. J.; Muckerman, J. T.; Himeda, Y.; Fujita, E. *Inorg. Chem.* **2013**, *52*, 12576−12586.
(42) Jeletic, M. S.; Mock, M. T.; Appel, A. M.; Linehan, J. C. *J. Am. Chem. Soc.* **2013**, *135*, 11533−11536.
(43) Getty, A. D.; Tai, C.-C.; Linehan, J. C.; Jessop, P. G.; Olmstead, M. M.; Rheingold, A. L. *Organometallics* **2009**, *28*, 5466−5477.
(44) Galan, B. R.; Schöffel, J.; Linehan, J. C.; Seu, C.; Appel, A. M.; Roberts, J. A. S.; Helm, M. L.; Kilgore, U. J.; Yang, J. Y.; DuBois, D. L.; Kubiak, C. P. *J. Am. Chem. Soc.* **2011**, *133*, 12767−12779.
(45) Quaranta, E.; Carafa, M.; Trani, F. *Appl. Catal., B* **2009**, *91*, 380−388.
(46) Kumar, N.; Camaioni, D. M.; Dupuis, M.; Raugei, S.; Appel, A. M. *Dalton Trans.* **2014**, *43*, 11803−11806.
(47) Bauer, W.; Ellermann, J.; Dotzler, M.; Pohl, D.; Heinemann, F. W.; Moll, M. *Z. Anorg. Allg. Chem.* **2000**, *626*, 574−587.
(48) Hong, F.-E.; Huang, Y.-L.; Chen, H.-L. *J. Organomet. Chem.* **2004**, *689*, 3449−3460.
(49) Dana, B. H.; Robinson, B. H.; Simpson, J. *J. Organomet. Chem.* **2002**, *648*, 251−269.
(50) Mirza, H. A.; Vittal, J. J.; Puddephatt, R. J.; Frampton, C. S.; Manojlovic-Muir, L.; Xia, W.; Hill, R. H. *Organometallics* **1993**, *12*, 2767−2776.
(51) Elliot, D. J.; Holah, D. G.; Hughes, A. N.; Magnuson, V. R.; Moser, I. M.; Puddephatt, R. J.; Xu, W. *Organometallics* **1991**, *10*, 3933−3939.
(52) Dietrich, J.; Schindler, S. *Z. Anorg. Allg. Chem.* **2008**, *634*, 2487−2494.
(53) Hutschka, F.; Dedieu, A.; Eichberger, M.; Fornika, R.; Leitner, W. *J. Am. Chem. Soc.* **1997**, *119*, 4432−4443.
(54) Mock, M. T.; Potter, R. G.; O'Hagan, M. J.; Camaioni, D. M.; Dougherty, W. G.; Kassel, W. S.; DuBois, D. L. *Inorg. Chem.* **2011**, *50*, 11914−11928.
(55) Qi, X.-J.; Fu, Y.; Liu, L.; Guo, Q.-X. *Organometallics* **2007**, *26*, 4197−4203.
(56) Curtis, C. J.; Miedaner, A.; Ellis, W. W.; DuBois, D. L. *J. Am. Chem. Soc.* **2002**, *124*, 1918−1925.
(57) DuBois, D. L.; Berning, D. E. *Appl. Organomet. Chem.* **2000**, *14*, 860−862.
(58) Kaljurand, I.; Kütt, A.; Sooväli, L.; Rodima, T.; Mäemets, V.; Leito, I.; Koppel, I. A. *J. Org. Chem.* **2005**, *70*, 1019−1028.
(59) Kisanga, P. B.; Verkade, J. G.; Schwesinger, R. *J. Org. Chem.* **2000**, *65*, 5431−5432.
(60) Schwesinger, R.; Hasenfratz, C.; Schlemper, H.; Walz, L.; Peters, E.-M.; Peters, K.; von Schnering, H. G. *Angew. Chem., Int. Ed. Engl.* **1993**, *32*, 1361−1363.
(61) Qi, X.-J.; Liu, L.; Fu, Y.; Guo, Q.-X. *Organometallics* **2006**, *25*, 5879−5886.
(62) Ciancanelli, R.; Noll, B. C.; DuBois, D. L.; Rakowski-Dubois, M. *J. Am. Chem. Soc.* **2002**, *124*, 2984−2992.
(63) Schunn, R. A. *Inorg. Chem.* **1970**, *9*, 2567−2572.
(64) Yonker, C. R.; Linehan, J. C. *J. Organomet. Chem.* **2002**, *650*, 249−257.
(65) Yonker, C. R.; Linehan, J. C. *Prog. Nucl. Magn. Reson. Spectrosc.* **2005**, *47*, 95−109.
(66) Dolomanov, O. V.; Bourhis, L. J.; Gildea, R. J.; Howard, J. A. K.; Puschmann, H. *J. Appl. Crystallogr.* **2009**, *42*, 339−341.
(67) Sheldrick, G. M. *Acta Crystallogr., Sect. A* **2008**, *64*, 112−122.